CORE
Metadata, citation and similar papers at core.ac.uk
Provided by NASA Technical Reports Server

IN-34
36819
p.13

NASA Technical Memorandum 105661

Modelling and Experimental Verification of a Water Alleviation System for the NASP

G. James Van Fossen
Lewis Research Center
Cleveland, Ohio

Prepared for the
92nd National Heat Transfer Conference
American Society of Mechanical Engineers
San Diego, California, August 9–12, 1992

NASA

(NASA-TM-105661) MODELLING AND EXPERIMENTAL VERIFICATION OF A WATER ALLEVIATION SYSTEM FOR THE NASP (NASA) 13 p CSCL 20D
N92-23224
Unclas
G3/34 0086819

MODELLING AND EXPERIMENTAL VERIFICATION OF A WATER ALLEVIATION SYSTEM FOR THE NASP

G. James Van Fossen

NASA Lewis Research Center
Cleveland, Ohio 44135

ABSTRACT

One possible low speed propulsion system for the National AeroSpace Plane is a Liquid Air Cycle Engine (LACE). The LACE system uses the heat sink in the liquid hydrogen propellant to liquify air in a heat exchanger which is then pumped up to high pressure and used as the oxidizer in a hydrogen-liquid air rocket. The inlet air stream must be dehumidified or moisture could freeze on the cryogenic heat exchangers and block them.

The main objective of this research has been to develop a computer simulation of the cold-tube/antifreeze-spray water alleviation system and to verify the model with experimental data. An experimental facility has been built and humid air tests were conducted on a generic heat exchanger to obtain condensing data for code development.

The paper describes the experimental setup, outlines the method of calculation used in the code, and presents comparisons of the calculations and measurements. Causes of discrepancies between the model and data are explained.

NOMENCLATURE

A_i, A_o	tube inside or outside surface area
C_d	proportionality constant between shear stress and velocity
C_p	heat capacity at constant pressure
C_1, C_2	constants in glycol distribution function (eqn. (15))
D_i, D_o	tube inside or outside diameter
H_{fg}	heat of vaporization of water
h	heat transfer coefficient
h_m	mass transfer coefficient
k	thermal conductivity
L	tube length
Le	Lewis number
$\dot{m}$	fluid flow rate
Q	dynamic pressure
q	heat flow
T	temperature
UA_{f-r}	overall heat conductance, film-air interface to refrigerant
V	velocity
W_{fog}	flow rate of fog per unit weight of dry air
W_0	flow rate of glycol/water mixture per unit weight of dry air from upstream tube rows that is captured by tube row under consideration
W_2	specific humidity of tube row outlet air stream
y	coordinate normal to tube surface

Greek symbols

δ	film thickness
Δp	pressure difference
ΔW	flow rate of water condensed per unit air flow
η_i	fraction of water/glycol mixture approaching tube row that is caught
μ	viscosity
ρ	fluid density
τ	shear stress

Subscripts

a	air
b	bulk or average condition
film, *f*	film of condensate on tube
fog	fog
i	tube row *i*
in	inlet
lat	latent heat
mix	water/glycol mixture
out	outlet
o	outside surface
r	refrigerant
sat	saturation conditions
sens	sensible heat
stm	steam
w	tube wall
∞	free stream conditions

INTRODUCTION

One possible low speed propulsion system for the National AeroSpace Plane (NASP) is a Liquid Air Cycle Engine (LACE). The LACE system uses the heat sink in the liquid hydrogen propellant to liquify air in a heat exchanger. The liquid air is then pumped up to high pressure and is used as the oxidizer in a hydrogen-liquid air rocket. The NASP will be required to operate from almost any location on earth; thus, humidities as high as 0.02 Kg-H_2O/Kg-air could be encountered. Moisture from the air could freeze on the cryogenic heat exchangers and block them. For this reason, the incoming air stream must be dehumidified before coming in contact with the cryogenic systems.

Any dehumidification system must operate with low pressure losses. High system pressure loss would require large heat exchanger face area in order to pass the required air flow thus increasing system weight and volume. In the condesing portion of the LACE system, as the air condensing pressure is lowered, its saturation temperature approaches its freezing temperature. Thus, a large pressure loss in the dehumidification system could cause the condenser unit to freeze with solid air. There are several practical ways to remove moisture from an air stream. Desiccant beds, freeze-out heat exchangers, and cold-tube heat exchangers are examples.

Desiccant beds remove moisture by passing the stream through a packed bed of moisture-absorbing material such as silica gel. For the NASP application this would be impractical because the water removed from the air would stay on board and increase system weight.

In the freeze-out method, moisture is removed by passing the humid air through a very cold heat exchanger. The moisture is deposited on the heat exchanger surface in the form of frost. The heat exchanger must be defrosted periodically or pressure loss becomes excessive and moisture removal efficiency decreases. For continuous operation a second identical heat exchanger can be employed while the frozen unit is deiced. This system requires valving to switch from cold refrigerant to a source of heat to defrost the ice laden unit. Valves must also be used to shuttle the air flow from one unit to the other.

The cold-tube/antifreeze-spray alleviation system works like a home dehumidifier. Moist air is passed over the tubes of a heat exchanger which are cooled below the dew-point temperature of the air stream. Water condenses on the tubes and is blown downstream in the form of droplets which are removed with a particle separator. An antifreeze can be sprayed on the face of the heat exchanger to prevent water freezing and allow refrigerant temperatures down to 222 K or lower. This is a continuous process and the pressure loss can be kept low.

The main objective of this research has been to develop a computer simulation of the cold-tube/antifreeze-spray water alleviation system. Toward this end, a computer code was developed, an experimental facility was built, and humid air data obtained for code development. The computer code can predict the heat flow, pressure loss, outlet air temperature, and the outlet humidity of the air stream given the air inlet conditions, heat exchanger geometry, and refrigerant inlet conditions. Refrigerant outlet conditions are also predicted.

This paper will describe the experimental facility and outline the method of calculation used in the computer code. The experimental data will be presented and a comparison with computer predictions will be made. Causes of discrepancies between the model and the data will be examined.

EXPERIMENTAL FACILITY

Air, steam and glycol systems - Figure 1 is a schematic representation of part of the experimental facility. Shown on the figure are the air, steam humidification, glycol spray, and condensate collection systems. Starting at the upper right of the figure, air at 275.8 KPa pressure with a dew point of about 233 K was passed through an orifice run and through the flow control-valve. At this

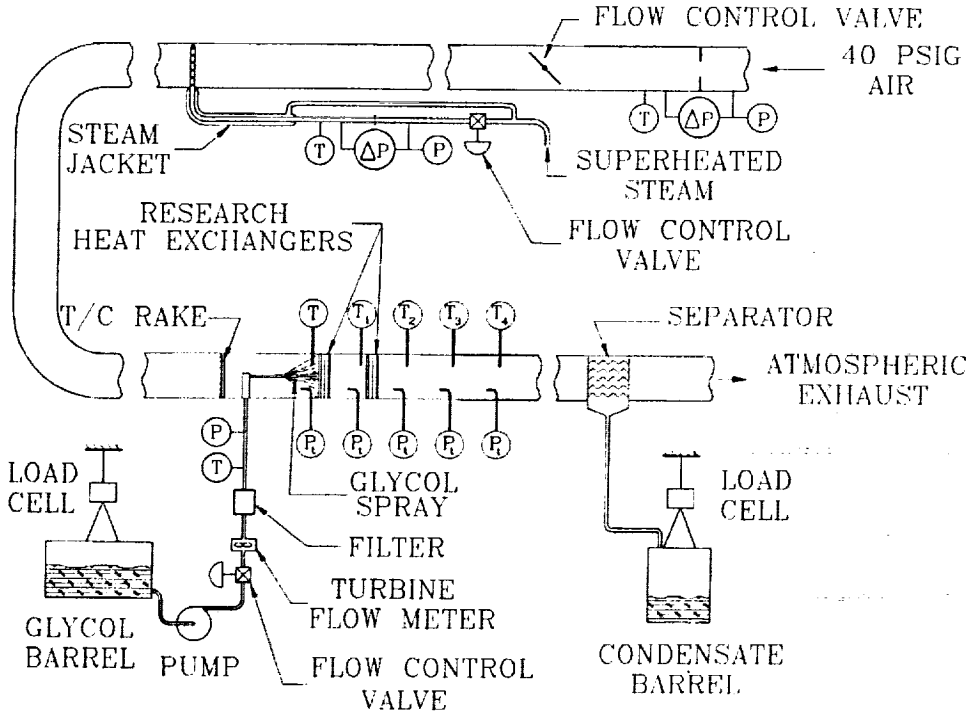

Figure 1. Air, steam, and glycol systems.

point steam with around 8°C of superheat was injected into the duct to humidify the air. An orifice run was also used to measure the steam flow. The amount of steam that could be added without producing fog was a function of the air supply temperature which in turn depended on ambient temperature. Maximum humidity obtained for these tests was around 0.021 lbm-H_2O/lbm-air (147 grains/lbm).

Air total pressures were measured upstream and downstream of each heat exchanger core. A cross rake of 16 thermocouples measured the incoming air temperature. Air temperatures were also measured downstream of each heat exchanger core with a single thermocouple that was shielded to prevent contact with the cold condensate-glycol mixture. The air and condensate-glycol mixture then passed through a wavy plate separator where the condensate-glycol mixture was removed. The separator was custom fabricated for this application with vanes similar to the Brugess-Manning inline vane series 3200. The condensate ran into a barrel that was suspended from a load cell which was used to determine the flow rate. Air then passed to atmospheric exhaust.

Ethylene glycol antifreeze was sprayed onto the face of the upstream heat exchanger. Two different glycol nozzles were used for these tests, they were the Bete Fog Nozzle, Inc. model numbers FWL-1/4-120X and FWL-1/2-120X. Both were 120° full cone nozzles with a square spray pattern. The glycol supply barrel was suspended from a load cell which was used to measure the flow rate. Antifreeze nozzle droplet size was measured for a limited number of flow conditions with a Malvern Particle Sizer Model 2600 HSD.

Refrigeration system - The research heat exchangers were cooled by circulating refrigerant R-12 through them. The refrigerant did not change phase as in a vapor compression cycle but stayed in the liquid state. The refrigerant was cooled by pumping it through a shell and tube heat exchanger with liquid nitrogen (LN_2) on the shell side as shown in figure 2. R-12 was chosen as a refrigerant because it has a freezing temperature around 117 K. This was still well above the temperature of boiling LN_2 (78 K) but the R-12 did not appear to freeze in the heat exchanger. Freezing did not occur because the heat exchanger tube wall temperature was above the Leidenfrost temperature of LN_2; this caused it to film boil which led to a large temperature rise across the nitrogen vapor film. R-12 temperatures were measured at the inlet and outlet of each of the research heat exchanger cores and flow rates were measured at the outlet of each core. These flow rates and temperatures were then used to calculate a heat flow rate which was compared to the air side heat flow rate.

Research heat exchangers - The heat exchanger cores shown in Figure 3 were fabricated from 0.125 inch diameter, bare (without fins), aluminum tubes with 0.020 inch wall thickness. The tubes were oriented vertically and arranged in an inline pattern with a tube

Figure 3. Research heat exchanger and air duct.

spacing of 1.25 tube diameters in the airflow direction and 1.5 diameters in the non-flow direction. The width or non-flow dimension of the heat exchanger duct was 12 inches and the duct height (tube length) was 12 inches. There were 64 tubes in each row and 20 tube rows in the airflow direction in each of the two cores. Tube stiffener sheets divided the duct into thirds. The tubes passed through clearance holes in the stiffener sheets but were not fastened to the stiffener sheets. The tubes were epoxied into the tube sheets. The R-12 inlet and outlet manifolds were bolted to the tube sheets and were sealed with "O" rings. The core-manifold assembly was

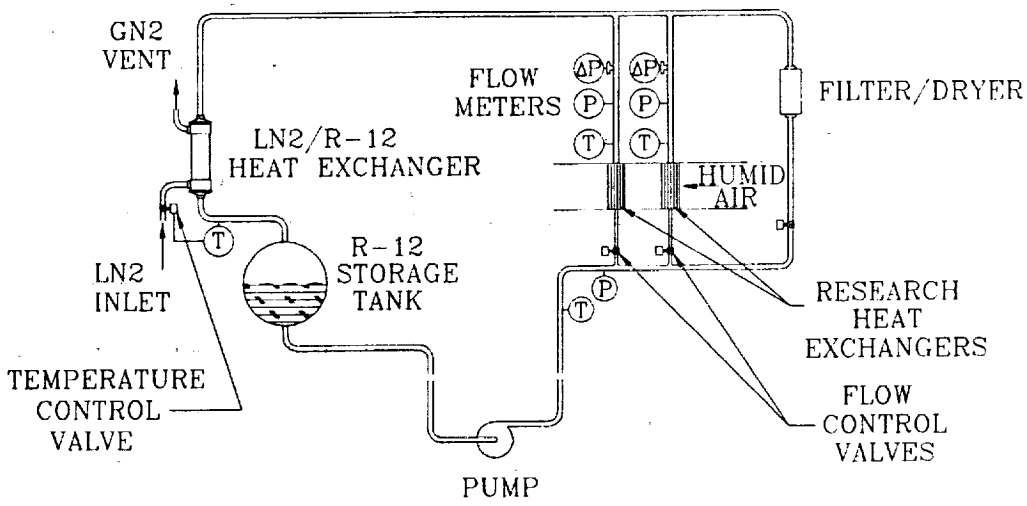

Figure 2. Refrigeration system.

ORIGINAL PAGE
BLACK AND WHITE PHOTOGRAPH

then installed into the air duct housings also shown in figure 3. The air duct housings separated each core by 3.5 inches; this allowed for instrumentation access between core segments. Tube vibration was a major problem as evidenced by grooves worn in the tubes at the stiffener sheet and cracking of the tubes at the tube sheet joints.

Figure 4 shows four heat exchanger cores installed in the rig; for the present test only the two upstream cores were in place. The refrigerant flow was kept the same through each of the two cores so they functioned as a single refrigerant pass. Humid air entered from the right and refrigerant (R-12) entered through the pipes on the bottom and exited at the top. The viewports were provided to observe the condensation, ice formation and runoff of water on the tubes.

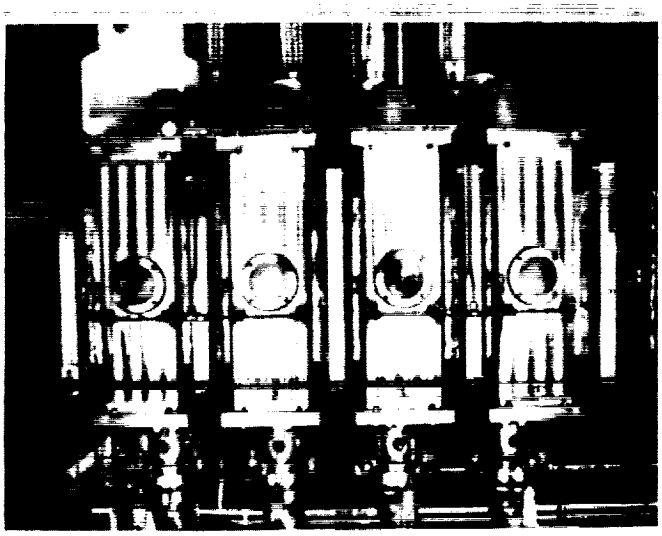

Figure 4. Research heat exchangers installed in rig.

DATA RECORDING

All data were recorded on the laboratory data acquisition system described in Ref. 1. To help eliminate some of the noise present in the system twenty "scans" or individual readings of each data channel were recorded. These twenty scans were then averaged to give a single reading for each channel and a statistical analysis was performed to give a variance for each channel which was used in the error analysis. A reading was taken about every 90 seconds and 8-12 readings were taken during each test run. Details of how calculated quantities were obtained from the measured values can be found in Ref. 2.

ERROR ANALYSIS

An error analysis was performed by assuming an appropriate fixed percentage error for each measuring instrument and adding to that the standard deviation computed for each reading. These assumed errors were then combined by the method of Kline and McClintock (Ref. 3) to obtain an error estimate for each calculated quantity. A table of error estimates for each reading is available in Ref. 2.

COMPUTER MODEL

Both air and refrigerant mass flows and inlet temperatures were assumed known as well as air inlet humidity; outlet temperatures, humidity, and pressure drops were calculated. Each core segment of the heat exchanger consisting of one refrigerant pass was solved from air inlet to exit, one tube row at a time; the air exit conditions for the first tube row became the inlet conditions for the second row and so on.

Hygroscopic Effect of Ethylene Glycol

Experimental results presented in Ref. 2 show that humidity could be removed from the air stream by the hygroscopic action of ethylene glycol. This effect was ignored in calculating the heat and mass balances for the dehumidifier for the following reasons. First, the overall energy balance will not be effected by the hygroscopic removal of water because the heat of condensation of water must still be removed by the heat exchanger. Second, very little water was removed by hygroscopic action due to low relative velocity between air and glycol and low surface area. Finally, the hygroscopic effect was shown to be effective only for pure ethylene glycol; thus, as water condenses and dilutes the glycol the hygroscopic potential will be lost after a few tube rows.

Heat and Mass Transfer

The following logic was used to determine if condensing water and frozen condensate were present: 1. The tube row average surface temperature was first calculated assuming no condensing took place. 2. If the resulting average tube temperature was below the dew-point temperature of the incoming air, the tube temperature was recalculated with a condensing water-ethylene glycol film on its surface. 3. If the resulting tube temperature with condensing was below the freezing temperature of the condensate-ethylene glycol mixture, the tube temperature could be recalculated with a layer of ice between the tube wall and the condensate film. This latter condition was not encountered experimentally and will not be discussed further. Calculation of dry heat transfer is straightforward; the calculation of heat transfer and pressure drop with condensing water and antifreeze-spray will now be discussed.

Initial guesses for the outlet temperatures of the air and refrigerant streams as well as the average tube surface temperature were made to start the calculation. Refrigerant temperature was taken to be an average value for each tube row which resulted in a constant tube surface temperature for each row. In addition to the unknown air and refrigerant outlet temperatures the temperature of the liquid-vapor interface where condensation takes place, T_{sat}, was unknown. This interface temperature controls the rate of diffusion of steam to the condensate surface. An initial guess of T_{sat} was also made to start the calculation. Heat flow was assumed constant along the tube length and was calculated from the equation

$$q = q_{sens} + q_{lat} \qquad (1)$$

The sensible heat or heat convected to the surface of the condensate film was calculated from

$$q_{sens} = h_a A_o (T_{a,b} - T_{sat}) \qquad (2)$$

h_a, the heat transfer coefficient between the air and tube bank, was calculated from a curve fit of the data in Ref. 4. The heat of

ORIGINAL PAGE
BLACK AND WHITE PHOTOGRAPH

condensation or latent heat is

$$q_{lat} = \dot{m}_a \, \Delta W \, H_{fg} \qquad (3)$$

where ΔW is the flow rate of steam that diffuses to the tube row per unit air flow.

The rate of condensation of water on the tubes is controlled by the diffusion of steam through air to the surface of the condensate film. The heat-mass transfer analogy was used to calculate the rate of steam diffusion. The mass transfer coefficient, h_m, was calculated from the heat transfer coefficient and the Lewis number, Le, as (Ref. 5):

$$h_m = \frac{h_a}{\rho_a \, C_{p,a} \, (Le)^{0.67}} \qquad (4)$$

Several data points were taken with the R-12 temperature above the freezing temperature of water in order to test the code with no glycol spray. Comparing these data with the calculated values it was determined that the dry heat transfer coefficient, h_a, must be multiplied by a factor of 1.18 when condensing is present. This augmentation is consistent with the findings of other authors (Ref. 6). The condensate flow rate was calculated from the mass transfer coefficient and the concentration gradient (steam density difference) between the free stream and the condensate surface.

$$\Delta W = \frac{h_m \, A_o (\rho_{stm,\infty} - \rho_{stm,sat})}{\dot{m}_a} \qquad (5)$$

The thickness of the condensate film was needed to calculate the film thermal conductance and the increase in pressure loss due to the increased blockage. It was found that Nusselt's falling film analysis (Ref. 7) of condensing on vertical tubes gave film thicknesses that were unrealistically large. His analysis did not account for the shearing effect of air flowing over the tubes. An analysis was made of the condensate film that assumed the film to be thin compared to the tube diameter, the shearing effect to be dominant and gravity terms could be ignored. This analysis is illustrated in figure 5. Velocity and temperature profiles in the film were assumed linear and shear stress at the edge of the film was assumed to be proportional to the air velocity.

$$\tau = \mu_{mix} \frac{dV_{mix}}{dy} = C_d \, \mu_a \frac{V_a}{D_o} \qquad (6)$$

The average film thickness, δ, was then determined to be

$$\delta = \frac{2}{3\pi A}\left[(A\pi + B)^{\frac{3}{2}} - B^{\frac{3}{2}}\right] \qquad (7)$$

Where A and B are defined by

$$A = \frac{\mu_{mix} \, D_o^2 \, h_m (\rho_{stm,\infty} - \rho_{stm,sat})}{\rho_{mix} \, C_d \, \mu_a V_a} \qquad (8)$$

$$B = \frac{\mu_{mix} \, W_o}{\rho_{mix} C_d \, \mu_a V_a} \qquad (9)$$

C_d is a constant; a value of 115 was found to give the best agreement between data obtained in these experiments and calculations. The film conductance, h_{film}, was calculated from the film thickness as

$$h_{film} = \frac{k_{mix}}{\delta} \qquad (10)$$

The overall heat transfer from the liquid-vapor interface to the refrigerant was calculated as

$$q_{f-r} = UA_{f-r}(T_{sat} - T_{r,b}) = \frac{(T_{sat} - T_{r,b})}{\frac{1}{h_{film} \, A_o} + \frac{\ln(\frac{D_o}{D_i})}{2\pi k_w \, L} + \frac{1}{h_r \, A_i}} \qquad (11)$$

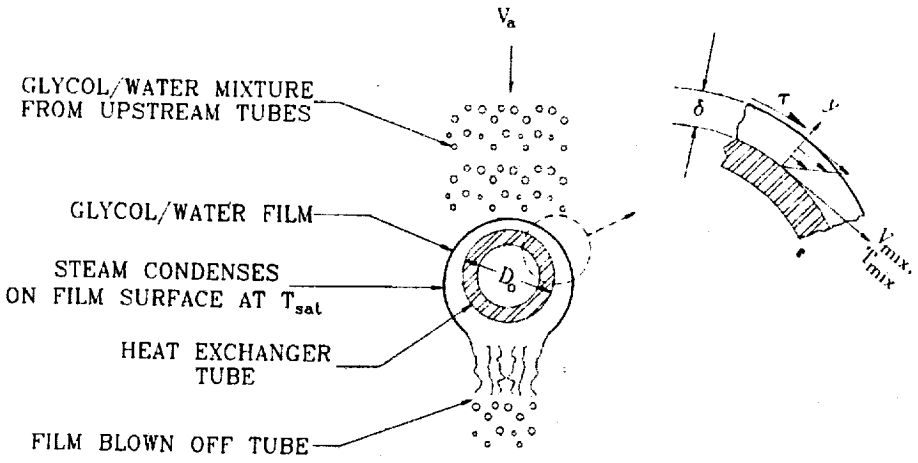

Figure 5. Glycol/Water film model.

Equating the heat flow between the air and the vapor-liquid interface, eqn. (1), and from the vapor-liquid interface to the refrigerant, eqn. (11), then gave a new estimate for the interface temperature .

$$T_{sat} = \frac{q_{lat} + UA_{f-r}T_{r,b} + h_a A_o T_{a,b}}{UA_{f-r} + h_a A_o} \qquad (12)$$

Fog Formation

The quantity of water condensed on a tube row was subtracted from the inlet steam flow to obtain a tube row outlet specific humidity. If the saturation value of humidity in the outlet stream was lower than the calculated outlet humidity, the excess was assumed to be converted into fog. This was an important consideration; if the condensation to fog was not accounted for, the predicted outlet air temperatures were too low. A new estimate of the air outlet temperature was obtained from an energy balance of the air, glycol, steam, condensate, and fog entering and leaving the tube row.

$$T_{a,out} = \frac{\Delta W(H_{fg}+C_{p,wv}(T_{a,in}-T_{sat}))+W_{fog}H_{fg,fog}+T_{a,in}(C_{p,a}+W_2C_{p,wv}+W_0C_{p,mix})-\frac{q}{\dot{m}_a}}{C_{p,a}+W_2C_{p,wv}+W_0C_{p,mix}} \qquad (13)$$

A new estimate of the tube wall temperature, $T_{w,o}$, was obtained by equating the heat conducted through the liquid film with the total heat transfer

$$T_{w,o} = T_{sat} - \frac{q}{h_{film} A_o} \qquad (14)$$

With these new estimates the procedure was repeated iteratively until the liquid-vapor interface and tube surface temperatures did not vary more than 0.03°C between iterations.

The refrigerant flow was assumed to be divided equally between the tube rows. The refrigerant enthalpy rise and outlet temperature were calculated from the heat flow and the refrigerant flow rate. Refrigerant exit temperatures for all the tube rows were then averaged to determine the outlet refrigerant temperature for the entire refrigerant pass.

Pressure loss

The effect of the condensate layer on air side pressure loss was accounted for by increasing the diameter of the tubes by twice the average thickness of the layer, which decreased the minimum free flow area of the tube bank. Pressure loss was calculated as recommended in Ref. 4 with the assumption that the liquid film did not alter the friction factor.

Antifreeze distribution

Ethylene glycol antifreeze was sprayed only on the face of the upstream heat exchanger. The assumed distribution of glycol on the downstream tube rows had a large effect on the calculated pressure loss; heat transfer results were less sensitive because the film conductance was relatively high. The glycol distribution was modeled by defining a "catch efficiency," η_i, as the fraction of glycol from upstream that hits tube row i. Condensed water from upstream was assumed to have the same catch efficiency as the glycol. A parabolic distribution of catch efficiency was assumed and the coefficients C_1 and C_2 were determined by matching the predicted pressure drop with the data of the present experiment. For the forty rows of tubes used in the present test, the catch efficiency was given by the equation

$$\eta_i = C_1\left(\frac{41-i}{40}\right)^2 + C_2 \qquad (15)$$

where i was the tube row numbered counted from the first upstream row, the best values for C_1 and C_2 were 0.1 and 0.5 respectively. All results presented in this paper used the glycol distribution model of equation (15).

EXPERIMENTAL RESULTS

Three groups of tests were run. In the first group there was essentially zero inlet humidity. These data were taken to validate the rig and data reduction procedures by comparing with calculations made with heat transfer and pressure drop correlations available in the literature for this tube bank configuration (Ref. 4). The main body of data was with humid air flowing over cold tubes and glycol spray to prevent water from freezing on the tubes. These data were obtained to aid in the development of the computer code. Finally, several runs were made to determine the amount of moisture that the ethylene glycol antifreeze could remove from the air stream due to its hygroscopic properties; hygroscopic results are reported in Ref. 2.

Energy Balance

Figure 6 is a comparison of the heat flow from the air stream and the heat flow into the refrigerant stream. For all the readings, the refrigerant heat flow is larger than the air heat flow. This was thought to be due to conditions in the refrigerant stream that caused local two phase flow at the heat exchanger exit even though the bulk conditions indicated the refrigerant was all liquid.

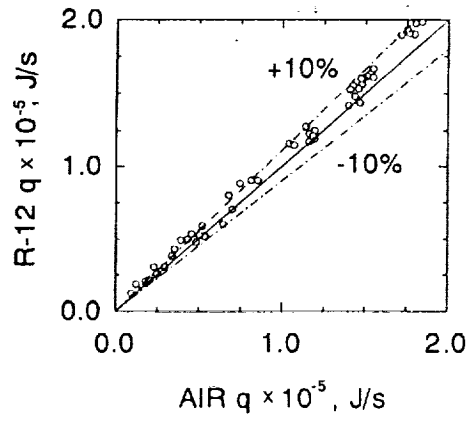

Figure 6. Comparison of R-12 and air heat flows.

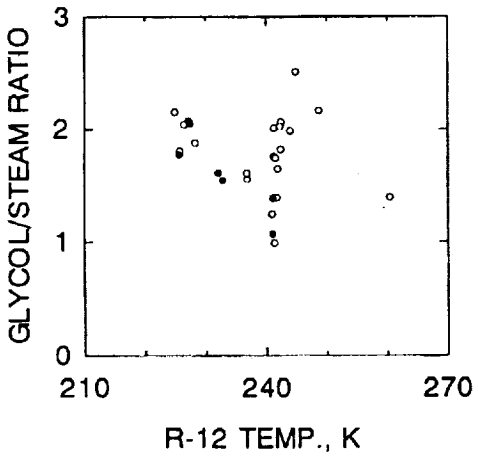

Figure 7. Experimental test matrix. Air flow, Kg/sec: closed symbols - 1.1; open symbols 1.8.

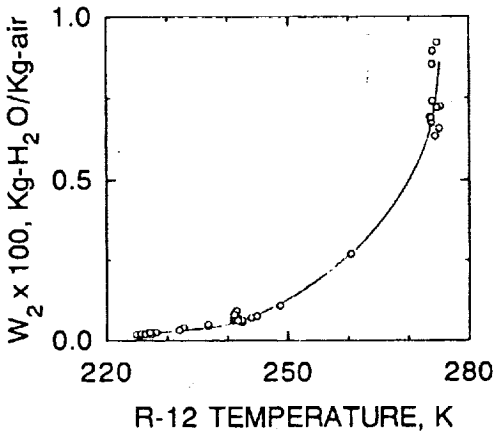

Figure 8. Measured outlet humidity as a function of R-12 inlet temperature.

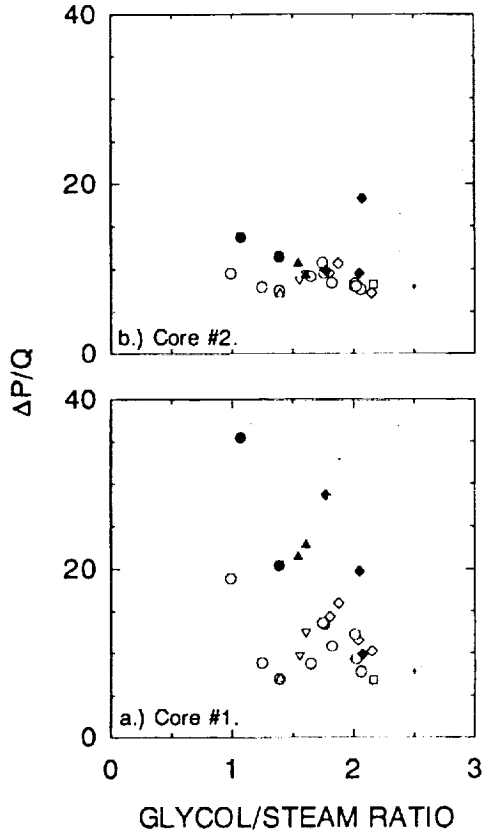

Figure 9. Dimensionless pressure drop as a function of glycol/steam ratio. Air flow, Kg/sec: closed symbols - 1.1, open - 1.8. Refrigerant temperature, K: ◇ - 224-228; ▽ - 232-233; ○ - 241-242; + - 244; □ - 249; △ - 261.

This led to high pressure loss across the refrigerant flow meter which caused a higher than actual flow rate to be calculated and thus the calculated refrigerant heat flow was too large. Heat gain from the surroundings could also have contributed to the imbalance. In general, the energy balance was within the estimated experimental error which gave confidence that the experimental setup was working properly.

Humid Air Heat Transfer Data

Test matrix. Figure 7 shows the experimental conditions that were run. Refrigerant temperatures ranged from 225 to 261 K; the ratio of glycol to steam flow ranged from 0.99 to 2.51. Two nominal air flows were run, they were 1.1 and 1.8 Kg/sec.

Outlet humidity. The outlet humidity was calculated from the measured air outlet temperature assuming saturated conditions. Figure 8 shows the outlet specific humidity as a function of refrigerant inlet temperature. The range of inlet humidity for these tests was from 0.0096 to 0.0212 Kg-H_2O/Kg-air. The lowest specific humidity obtained was 0.00018 Kg-H_2O/Kg-air; the inlet humidity for this data point was 0.0139 Kg-H_2O/Kg-air, and the refrigerant temperature was 225 K. The outlet air temperature for this point was 242 K. The shape of the curve is an indication of the diminishing returns that are obtained with lowering refrigerant temperature; to lower humdity further, more tube rows could be added.

Pressure loss. The dimensionless pressure loss ($\Delta p/Q$) across each heat exchanger core is shown in figure 9 plotted against glycol/steam ratio. One thing becomes immediately obvious; there is a large scatter in the pressure loss data for the first heat exchanger core, fig. 9 a.). There is a definite trend with air flow; the lower air flow has the higher dimensionless pressure loss. In general, pressure loss tends to decrease with increasing glycol/steam ratio and is higher for the lower refrigerant temperatures. The cause of the scatter will be discussed later. Examination of pressure loss for heat exchanger core #2, fig. 9 b.) reveals considerably less scatter; in fact, the dimensionless pressure loss appears nearly constant. The single anomalous point near glycol/steam ratio of 2 was for a special test which will be discussed later.

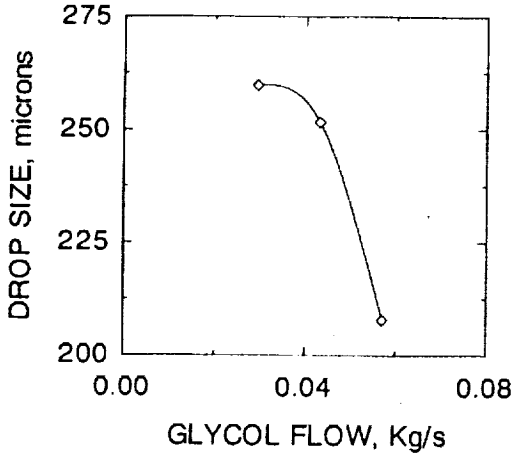

Figure 10. Antifreeze nozzle droplet size.

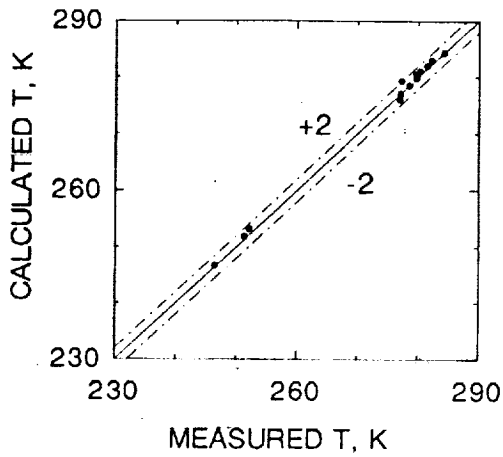

Figure 12. Comparison of measured and predicted air outlet temperature for dry air.

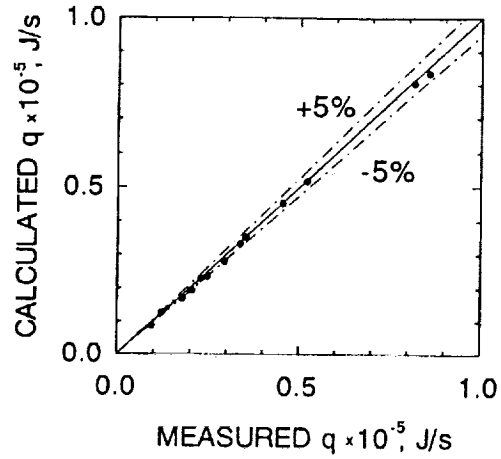

Figure 11. Comparison of measured and predicted heat flow, dry heat transfer.

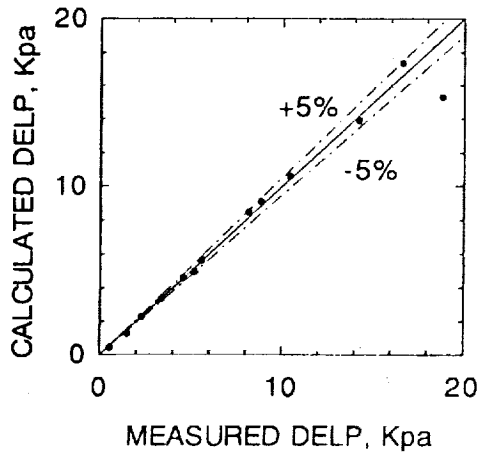

Figure 13. Comparison of measured and predicted pressure drop, no condensing.

Antifreeze nozzle droplet size. Nozzle droplet size was measured for the FWL-1/2-120X nozzle only. Figure 10 shows the median droplet diameter versus flow rate for room temperature ethylene glycol. For glycol flows between 0.06 and 0.12 lbm/sec the median diameter varied from 260 to 210μm.

COMPARISON OF EXPERIMENTAL DATA WITH CALCULATIONS

Dry Heat Transfer

The code was used to calculate heat transfer and pressure drop for the dry data by setting the inlet humidity to zero. Predicted heat flow, air outlet temperature, and pressure loss are compared with experimental data in figures 11-13. Agreement between the code and experimental data is within the estimated experimental accuracy.

Heat Transfer With Condensing Water

Figures 14-17 show a comparison of the experimental heat flow, outlet air temperature, condensate-glycol flow, and pressure loss for upstream (core #1) and downstream (core #2) heat exchanger cores versus the computer prediction for all the condensing data. Data were obtained both with a single 3 inch heat exchanger core and with two 3 inch cores cooled. The calculated heat flow agrees with the measured heat flow to within about 5% as seen on figure 14. Calculated air outlet temperatures agree within 3°C and calculated condensate flows (water + glycol) are also within 5% of the measured values. Note that the predicted condensate flow is high by about 3% over the range of the data. This may reflect inefficiency in the particle separator.

Pressure loss for the upstream core was not predicted successfully. The numerical results were generally too low. As seen on fig. 17 a.), the code predicted basically two levels of pressure loss reflecting the two experimental air flow rates; however, measured pressure losses had large scatter. Pressure loss predictions for the downstream core are much improved and are within +7 to -20%.

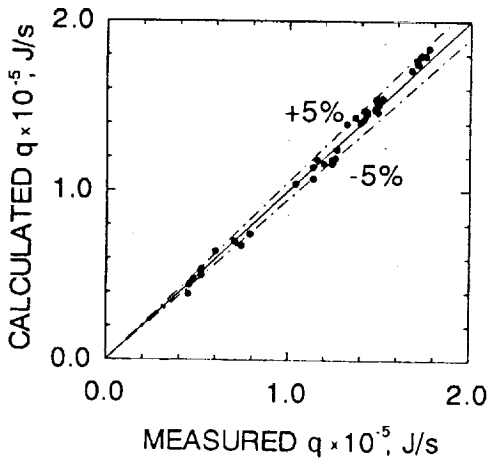

Figure 14. Comparison of measured and predicted heat flow with condensing.

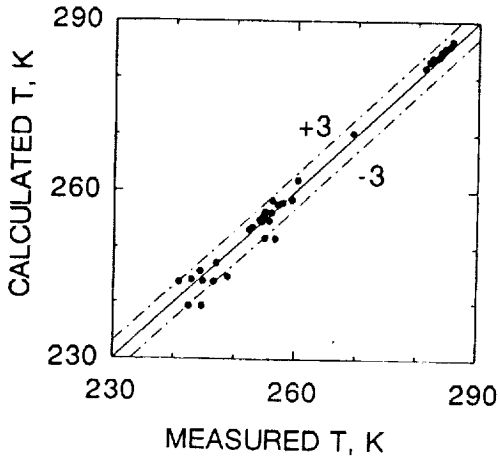

Figure 15. Comparison of measured and predicted air outlet temperature with condensing.

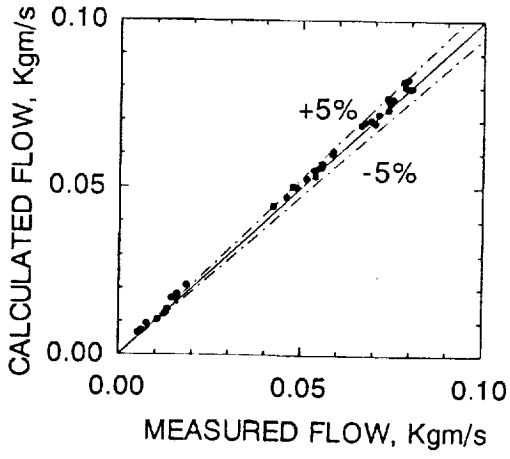

Figure 16. Comparison of measure and predicted condensate flow.

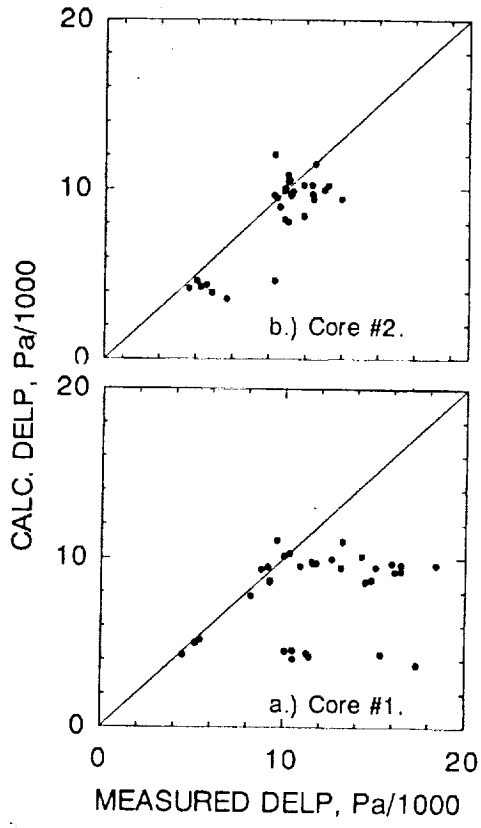

Figure 17. Comparison of measured and predicted air pressure drop with condensing.

To explain this discrepancy between the predicted and measured pressure loss examine figure 18. The total pressure measured upstream of each heat exchanger core as a function of time for one test run is shown in the figure. The downstream pressure remained constant at slightly above atmospheric (pressure loss across the separator was generally around 0.25 psi), thus the upstream total pressure was directly proportional to pressure loss through the core. At point **A**, the air and steam flows have been established with no refrigerant flow through the heat exchangers. At point **B**, a test glycol spray was started to set the proper glycol flow rate; the spray lasts approximately one minute. The resulting blip in the pressure trace was due to the liquid layer on the tubes that increased the blockage of the heat exchanger core. At point **C** the steam flow was turned off; this resulted in a slight drop in both mass flow and air temperature which caused the pressure loss to decrease. At point **D**, the refrigerant valve was opened and the heat exchangers began to cool off which caused the pressure to drop further. The steam and glycol flows were started simultaneously at point **E**; pressure then rose during the entire test run until point **F** where the steam and glycol flows were turned off. Of particular interest is the magnitude of the pressure decrease at point **F** when the steam and glycol flows were turned off. This pressure decrease was due to the liquid being blown off the tubes. It is only slightly larger than the decrease when the glycol test spray was turned off at point **B**; the difference is probably due to the colder temperature of the glycol at point **F** making it more viscous and thus increasing the liquid layer thickness.

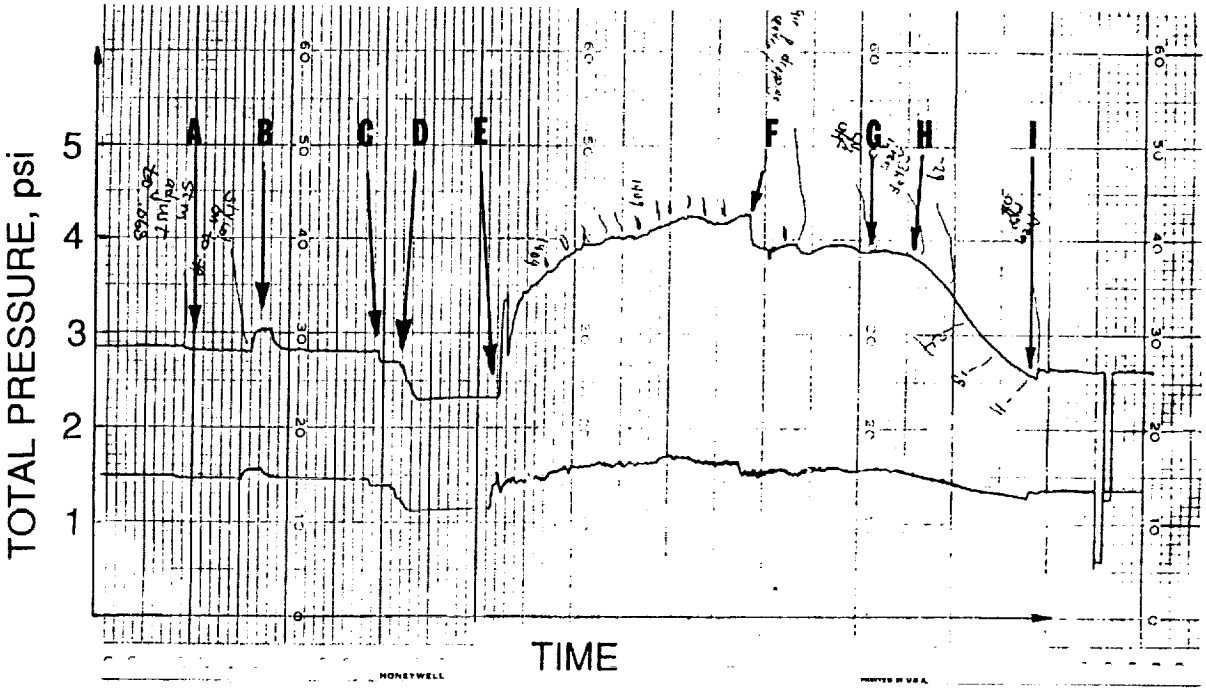

A- Heat exchanger at room temperature, air flow = 1.81 Kg/sec, steam flow = 0.025 Kg/sec, humidity = 1.37%.
B- Glycol test spray, heat exchanger at room temp., glycol flow rate = 0.045 Kg/sec, glycol/steam ratio = 1.8, pressure drop increases by ≈ 1.7 KPa.
C- Steam flow off.
D- Refrigerant valve to heat exchanger opened, T_r = 225 K.
E- Steam and glycol valves opened, pressure rises during entire test from **E** to **F**.
F - Steam and glycol valves closed, pressure drop decreases by ≈ 2.1 KPa and stays level between **F** and **G**.
G- LN_2 to cool refrigerant turned off - refrigerant begins to warm.
H- Refrigerant inlet temperature reaches ≈ 236 K, air pressure drop starts to decrease.
I - Refrigerant pump turned off.

Figure 18. Pressure history for a typical test run.

At point **G** the LN_2 to the refrigerant-LN_2 heat exchanger was turned off and the refrigerant began to warm up. The inlet temperature of the refrigerant reached 236 K at point **H** where the pressure began to fall. The pressure decreased toward the initial condition and the refrigerant pump was turned off at point **I**. The high pressure between points **F** and **H** must be due to something frozen on the tubes.

Calculations indicate that for any reasonable assumption of glycol distribution through the heat exchanger, the concentration of glycol in the glycol-water mixture will be such that no freezing can take place. The sketch in figure 19 illustrates what we believe happened to cause the large and erratic pressure losses in the first core. During initial checkout runs, the glycol nozzle streamwise position was adjusted until no visible frost appeared on the heat exchanger face. The nozzle had a square spray pattern but some overspray was observed when full coverage was obtained. Pure ethylene glycol freezes around 260 K. As shown in the sketch, the glycol rich overspray flows downstream onto the cold heat exchanger tubes and tubesheet where it freezes. This process continues throughout the entire run, increasing the frozen glycol layer thickness and thus increasing the pressure loss. No ice or frost was seen on the heat exchanger face; however, ice or more precisely slush was seen on the tubes next to the wall through the side

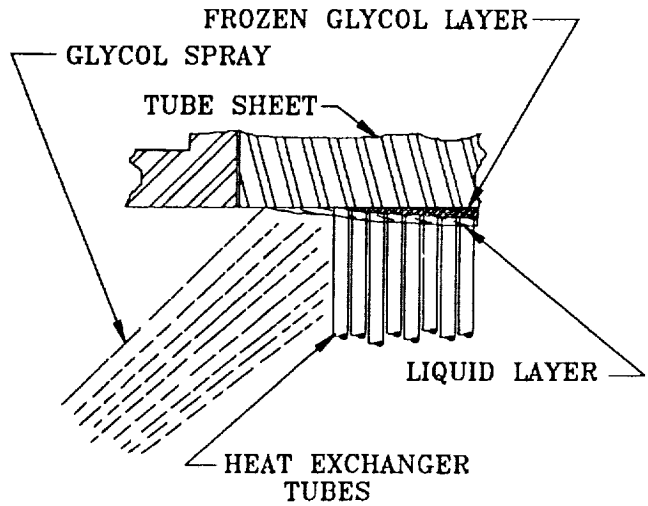

Figure 19. Pure glycol freezes near wall.

viewports during most runs. Calculations show that a 1/4-inch thick ice layer around the perimeter of the duct could account for a pressure loss of the magnitude observed between points G and I on Fig. 18.

In an attempt to eliminate the glycol rich overspray near the side walls, a 1-inch thick honeycomb with 1/4-inch cells was placed between the glycol nozzle and the face of the heat exchanger. The purpose of the honeycomb was to straighten the flow from the glycol nozzle and turn it parallel to the wall thus eliminating the overspray. The nozzle axial position was adjusted to provide full coverage to the honeycomb. The honeycomb did not lower the pressure loss in the first core and made the pressure loss in the second core higher as shown by the anomalous point on figure 9 b.). The honeycomb did turn the spray but also acted as an agglomerator making large glycol droplets from the small ones. Apparently, the large droplets did not reach the tubes on the downstream core and water froze on the tubes thus increasing the pressure drop.

SUMMARY OF RESULTS

Tests were conducted on a cold-tube water alleviation system that utilized ethylene glycol antifreeze to allow operation at subfreezing temperatures. A computer code was written and predictions were compared to the experimental data. The main results were:

1. The system was tested at refrigerant temperatures as low as 225 K and was found to be capable of lowering the humidity to 0.00018 Kg-H_2O/Kg-air.

2. The system air pressure loss increased during the test runs and was believed to be caused by the freezing of relatively pure glycol near the sidewalls due to nozzle overspray.

3. Large glycol drops were ineffective in reaching downstream tube rows causing water to freeze on the tubes and increasing the pressure drop.

4. Good agreement between experimental data and computer prediction was obtained for heat flow, outlet temperature, and condensate flow rate. Pressure loss was under predicted in the first core because of freezing of glycol due to non-ideal glycol distribution. Pressure loss predictions were improved in the second core and were within +7 to -20%.

CONCLUDING REMARKS

The objective of this work was to develop a computer model of a cold-tube water alleviation system that utilized ethylene glycol antifreeze to allow operation at reduced temperatures. Toward that end, an experimental rig was built and data taken at refrigerant temperatures down to 225 K. A successful computer model has been developed and can be used to explore possible design variations of the system. Great care must be taken in spraying the antifreeze on the heat exchanger; oversprays and droplet size have a large effect on the system pressure loss.

REFERENCES

1. Miller, R. L., "ESCORT: A Data Acquisition and Display System to Support Research Testing," NASA TM-78909, May 1978

2. Van Fossen, G. J., "Performance Testing and Modelling of a Water Alleviation System," NASP TP 1001, November 1991

3. Kline S. J., McClintock, F. A., "Describing Uncertainties in Single Sample Experiments," Mechanical Engineering, Vol. 75, No.1, Jan. 1953, pp3-8.

4. Kays, W. M., London, A. L., *Compact Heat Exchangers*, The National Press, Palo Alto, CA, 1955, Figure 52 page 93

5. Holman, J. P., *Heat Transfer*, Fourth Edition, McGraw-Hill Book Co., 1976, p 436

6. Tree, D. R., Helmer, W. A., "Experimental Heat and Mass Transfer Data for Condensing Flow in a Parallel Plate Heat Exchanger," ASHRAE Trans., Vol.82, pt.1, 1976, p289-299

7. Butterworth, D., *Heat Exchanger Design Handbook*, Hemisphere Pub. Corp., 1983, sections 2.6.1-2.6.3

REPORT DOCUMENTATION PAGE

Form Approved
OMB No. 0704-0188

Public reporting burden for this collection of information is estimated to average 1 hour per response, including the time for reviewing instructions, searching existing data sources, gathering and maintaining the data needed, and completing and reviewing the collection of information. Send comments regarding this burden estimate or any other aspect of this collection of information, including suggestions for reducing this burden, to Washington Headquarters Services, Directorate for information Operations and Reports, 1215 Jefferson Davis Highway, Suite 1204, Arlington, VA 22202-4302, and to the Office of Management and Budget, Paperwork Reduction Project (0704-0188), Washington, DC 20503.

1. AGENCY USE ONLY (*Leave blank*)	2. REPORT DATE	3. REPORT TYPE AND DATES COVERED
	August 1992	Technical Memorandum

4. TITLE AND SUBTITLE

Modelling and Experimental Verification of a Water Alleviation System for the NASP

5. FUNDING NUMBERS

WU-763-22

6. AUTHOR(S)

G. James Van Fossen

7. PERFORMING ORGANIZATION NAME(S) AND ADDRESS(ES)

National Aeronautics and Space Administration
Lewis Research Center
Cleveland, Ohio 44135-3191

8. PERFORMING ORGANIZATION REPORT NUMBER

E-7026

9. SPONSORING/MONITORING AGENCY NAMES(S) AND ADDRESS(ES)

National Aeronautics and Space Administration
Washington, D.C. 20546-0001

10. SPONSORING/MONITORING AGENCY REPORT NUMBER

NASA TM-105661

11. SUPPLEMENTARY NOTES

Prepared for the 92nd National Heat Transfer Conference sponsored by the American Society of Mechanical Engineers, San Diego, California, August 9-12, 1992. Responsible person, G. James Van Fossen, (216) 433-5892.

12a. DISTRIBUTION/AVAILABILITY STATEMENT

Unclassified - Unlimited
Subject Category 34

12b. DISTRIBUTION CODE

13. ABSTRACT (*Maximum 200 words*)

One possible low speed propulsion system for the National AeroSpace Plane is a Liquid Air Cycle Engine (LACE). The LACE system uses the heat sink in the liquid hydrogen propellant to liquefy air in a heat exchanger which is then pumped up to high pressure and used as the oxidizer in a hydrogen-liquid air rocket. The inlet air stream must be dehumidified or moisture could freeze on the cryogenic heat exchangers and block them. The main objective of this research has been to develop a computer simulation of the cold-tube/antifreeze-spray water alleviation system and to verify the model with experimental data. An experimental facility has been built and humid air tests were conducted on a generic heat exchanger to obtain condensing data for code development. The paper describes the experimental setup, outlines the method of calculation used in the code, and presents comparisons of the calculations and measurements. Causes of discrepancies between the model and data are explained.

14. SUBJECT TERMS

Heat transfer; Mass transfer; Condensing

15. NUMBER OF PAGES

12

16. PRICE CODE

A03

17. SECURITY CLASSIFICATION OF REPORT	18. SECURITY CLASSIFICATION OF THIS PAGE	19. SECURITY CLASSIFICATION OF ABSTRACT	20. LIMITATION OF ABSTRACT
Unclassified	Unclassified	Unclassified	